The Risk of Image Generator-Specific Traces in Synthetic Training Data

Georg Wimmer*[a], Dominik Söllinger*[b] and Andreas Uhl[c]
Paris Lodron University Salzburg, Jakob-Haringer-Str. 2, 5020 Salzburg, Austria

Keywords: Image Synthesis, GAN, Diffusion Model, Synthetic Artifacts.

Abstract: Deep learning based methods require large amounts of annotated training data. Using synthetic images to train deep learning models is a faster and cheaper alternative to gathering and manually annotating training data. However, synthetic images have been demonstrated to exhibit a unique model-specific fingerprint that is not present in real images. In this work, we investigate the effect of such model-specific traces on the training of CNN-based classifiers. Two different methods are applied to generate synthetic training data, a conditional GAN-based image-to-image translation method (BicycleGAN) and a conditional diffusion model (Palette). Our results show that CNN-based classifiers can easily be fooled by generator-specific traces contained in synthetic images. As we will show, classifiers can learn to discriminate based on the traces left by the generator, instead of class-specific features.

1 INTRODUCTION

Large amounts of publicly available data are the basis for training deep neural networks. To properly train a neural network, huge amounts of annotated training data are necessary. Of course, gathering such amounts of data is time consuming and expansive. A potential solution to that problem is to generate synthetic data (Man and Chahl, 2022). With the emergence of versatile and powerful new approaches like generative adversarial networks (GAN) and diffusion models (DM) that are able to generate photo-realistic images, synthetic image generation has become a hot topic in science. There are different approaches to using synthetic data for training deep neural networks. They range from using synthetic data only for certain classes (e.g. to remove class imbalances (Elreedy and Atiya, 2019)) to a general mixture of real and synthetic training data for all classes (categories) to the exclusive use of synthetic data.

An often raised question is how closely synthetic data resembles real data and whether the synthetic data are suited to train or improve a neural network. Recent work in various fields like e.g. medical imaging (Torfi et al., 2022; Chen et al., 2022), face recognition (Qiu et al., 2021; Zhang et al., 2021) and object detection (Li et al., 2022) show the potential of using synthetic data. On the other hand, mostly driven by the need to detect deep fakes, some work (Wesselkamp et al., 2022) has also shown that image synthesis methods leave unique artifacts in the image domain that are not contained in the real data. Hence, it can be argued that as long as such artifacts are present, synthetic images do not perfectly resemble real data. Such generator-specific traces might not be an issue for applications where the images across all categories (classes) are generated from the same image synthesis method (as e.g. in face recognition). However, we hypothesize that generator-specific traces can cause severe problems if deep learning based classifiers are trained using synthetic images, where different classes are generated using different image generators. The same may apply for classifiers that are trained using a mixture of real and synthetic data, if specific classes of the training data are only represented by synthetic data from a given generator (e.g. class 1 = synthetic, class 2 = real). For example, we might encounter such scenarios in the field of medical image analysis where a lack of data is an immanent problem as data cannot be easily shared due to privacy concerns. Additionally, there is often a lack of data for specific classes of images. Therefore, it might be tempting to increase the number of images with synthetic data. If a deep learning based classifier is now trained on both real and synthetic data (e.g., class 1 = synthetic and class 2 = real), it may learn to

[a] https://orcid.org/0000-0001-5529-0154
[b] https://orcid.org/0000-0002-4262-9195
[c] https://orcid.org/0000-0002-5921-8755
*These authors contributed equally

Wimmer, G., Söllinger, D. and Uhl, A.
The Risk of Image Generator-Specific Traces in Synthetic Training Data.
DOI: 10.5220/0012420600003660

In *Proceedings of the 19th International Joint Conference on Computer Vision, Imaging and Computer Graphics Theory and Applications (VISIGRAPP 2024) - Volume 3: VISAPP*, pages 199-206
ISBN: 978-989-758-679-8; ISSN: 2184-4321

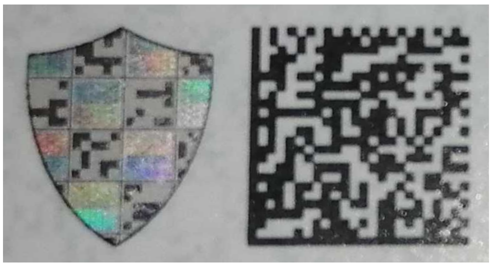

Figure 1: Example of a security label.

discriminate based on the traces left by the generator, which may provide a perfect decision boundary. The same applies if the classifier is trained using only synthetic data (e.g., class 1 = synthetic (generator A) and class 2 = synthetic (generator B)).

In this work, we therefore investigate whether the aforementioned hypothesis indeed poses an issue based on a scenario we encountered in industry. The detection of genuine and counterfeit "security labels" based on synthetically generated security labels. To the best of our knowledge, no previous work has investigated the effect of generator-specific traces (e.g., artifacts) on classifiers that are trained using synthetic images.

2 PRODUCT AUTHENTICATION BASED ON SECURITY LABELS

In order to stop product counterfeiting, the company "Authentic Vision" [1] offers security labels that can be attached to a product or its packaging. One example of such a security label can be seen in Figure 1. Each label features a hologram with a unique random pattern and multiple security features to prevent the security label from being replicated. For instance, the holographic foil shows reflections when exposed to light. Hence, missing reflections indicate forgery. Additionally, removing the security label exposes a diagonal, grid-like pattern which is referred to as the VOID pattern. Examples of security labels with a clearly visible VOID pattern can be found in Figure 2(c) and (f). Once the VOID pattern becomes visible, the product cannot be considered genuine. Note that in some cases, the VOID pattern is fairly hard to detect, in particular in cases where the VOID pattern only appears at small parts of the label. In order to verify whether a product is genuine or not, users can scan the security label with a smartphone app, which then performs all necessary checks to verify whether the product is genuine.

In order to verify whether a VOID pattern is visible or not, a convolutional neural network (CNN) is employed. This VOID pattern detector is trained on thousands of manually annotated security label scans in order to reliably detect scans with VOID patterns. As a result, changing key characteristics of the security label, such as its shape, can be challenging since new training data must first be gathered in order to retrain the model.

A potential solution to speed up the tedious task of manually collecting and annotating security labels is the use of synthetic data. One way to approach this task is by synthesizing environmental-specific characteristics (e.g., reflections, over-/underexposure, image blur), onto previously unseen labels (which might have a different shape).

In this work, we analyze whether synthetic data is a viable solution for that problem. This is done by comparing the results of the VOID pattern detector using either synthetic, real or mixed data to train the detector.

3 EXPERIMENTAL SETUP

3.1 Dataset

The dataset utilized in this work is composed of two types of images: enrollment images and scan images. Enrollment images are images of a security label that were captured in the factory. On the other hand, scan images are images of a security label captured in the real world (from users that scan the security label with the smartphone app). Since each security label is unique, each scan image can be uniquely assigned to an enrollment image. For every enrollment image, there is at least one scan image in the dataset. Examples of two enrollment images and their corresponding scan images can be observed in Figure 2 (top row). In total, there are 43517 enrollment images and 289309 scan images which exhibit a resolution of 165×189 pixel. Each of the scan image has been labeled as either genuine (class 'AUTH') or counterfeit (class 'VOID'). Note that all images underwent an initial prealignment to ensure that the hologram is perfectly aligned at the image center. Due to the prealignment, extracting a patch of size 128×128 from the image center results in an image that shows the hologram but almost no background. An example of such center-cropped enrollment and scan images can be found in Figure 2 (bottom row).

In order to validate the performance of the VOID pattern detector (described in Sec. 3.3) on scan images that have not been used for the training of the

[1] https://www.authenticvision.com/

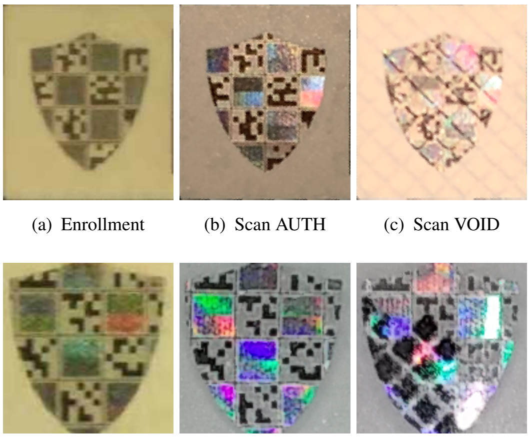

(a) Enrollment (b) Scan AUTH (c) Scan VOID

(d) Enrollment (e) Scan AUTH (f) Scan VOID

Figure 2: Examples of enrollment and scan images. Each row shows an original enrollment image (left) as well as a corresponding authentic scan (center) and void image (right). The bottom row shows the center-cropped version of the same enrollment and scan images.

detector nor the image synthesis methods (Sec. 3.2), the dataset is split into two sets: A training set composed of ∼ 90% of the enrollment images and the corresponding scan images, and a test set composed of the remaining ∼ 10% of the enrollment images and the corresponding scan images. As a result, the training set has 39193 enrollment and 259871 scan images (240075 Authentic + 19796 VOID). We further denote the Authentic (AUTH) scan images and their corresponding enrollment images from the training set as AUTH training set and the VOID scan images and their corresponding enrollment images from the training set as VOID training set. The test set has 4324 enrollment and 29438 scan images (26990 AUTH + 2448 VOID).

3.2 Synthetic Image Generation

We employ two different DL-based methods for conditional multi-modal image synthesis. The first method is based on a GAN, and the second model is based on a diffusion model. Both methods are employed to generate scan images based on enrollment images as input. The methods are trained using image pairs, where one image is an enrollment image and the other image a corresponding scan image. Both methods are once trained to generate Authentic scan images (using paired data from the AUTH training set) and once trained to generate VOID scan images (using paired data from the VOID training set).

A brief description of the employed architectures can be found in the following.

BicycleGAN. BicycleGAN (Zhu et al., 2017) (B-GAN) is a GAN-based conditional image generator for image-to-image translation. An advantage of the BicycleGAN model compared to most other DL-based image generation methods is its ability to produce both diverse and visually appealing results. This is achieved by learning an invertible mapping between the output of a generator (a scan image) and an 8-dimensional latent code, so that different latent code vectors actually lead to different outputs. The style of the scan images is encoded in the low-dimensional latent vector, which can be randomly sampled at test time. We use the implementation available at this website[2]. The BicycleGAN model is trained for 60 epochs with a batch size of 2. To fit the size of the images to the BicycleGAN's required image size, the training images (both enrollment and scan images) are first made quadratic ($165 \times 189 \rightarrow 189 \times 189$) by adding black background at the left and right side of the images, and then scaled to the size 256×256. Finally, the generated synthetic scan images are downsized ($256 \times 256 \rightarrow 189 \times 189$) and the black background is removed ($189 \times 189 \rightarrow 165 \times 189$). All enrollment images were initially transformed to grayscale. Grayscale conversion and the described resizing method led to the best results, in the author's opinion (we tested a lot of different configurations to find the best working one).

Palette. Palette (Saharia et al., 2022a) (P-DM) is an image-to-image diffusion model. An image-to-image diffusion model is a conditional diffusion model of the form $p(y|x)$, where x and y are images. In our case, x is an enrollment image and y is a scan image. For the diffusion process, Palette uses a U-Net architecture (Ho et al., 2020) with several modifications inspired by recent work (Dhariwal and Nichol, 2021; Saharia et al., 2022b; Song et al., 2020). Note that unlike in the original work, we train the network on 128×128 sized images (center-cropped from the enrollment and scan images) to reduce the quite substantial learning and inference time. We use the implementation available at this website[3]. The Palette Authentic image synthesizer is trained on AUTH training set for 240k iterations with a batch size of 64. The VOID image synthesizer is trained on VOID training set for 354k iterations with a batch size of 64. Random horizontal flipping is applied to increase the number of samples in the training set.

[2] https://github.com/junyanz/BicycleGAN

[3] https://github.com/Janspiry/Palette-Image-to-Image-Diffusion-Models

3.3 CNN-Based VOID Pattern Detector

In order to assess the ability of the synthetic data to replace real data, a CNN-based VOID pattern detector is trained to differentiate genuine scan images (AUTH images) from counterfeits (VOID images). An EfficientNet-B0 (Tan and Le, 2019) pretrained on ImageNet is utilized for this purpose. The model is trained to distinguish AUTH from VOID samples using a binary cross entropy loss. Thanks to the pretrained model, training with an ADAM optimizer (learning rate $lr = 10^{-4}$, weight decay $w = 10^{-3}$ and batch size $b = 64$) for only 3000 iterations is sufficient to achieve model convergence. Furthermore, note that there is a significant class imbalance between the number of scan images of the AUTH training set and the VOID training set. In order to overcome this issue, we applied weight sampling to make sure that images of each class have the same likelihood of being shown to the model.

3.4 Evaluation Protocol

To analyze the impact of the employed training data on the accuracy of the VOID pattern detector, we conduct experiments with the following training data compositions:

- Real world scan images from the AUTH (∼240k images) and VOID training set (∼20k images). This is the baseline accuracy.
- Real world scan images from the VOID training set (∼ 20k images) and synthetic scan images from class AUTH (50k images). This data composition is motivated by the possibly too low number of training samples from the VOID training set to properly train the image synthesis methods.
- Synthetic images from both classes (50k images per class)

In order to generate synthetic training data for the AUTH and VOID class, separate models are trained for each class (AUTH and VOID) and architecture (B-GAN and P-DM). We generate a set of 50k synthetic images for each class. The synthetic images of class Authentic are generated from 10k enrollment images from the AUTH training set (5 scan images per enrollment image) and the synthetic images of class VOID are generated from 1k enrollment images from the VOID training set (50 scan images per enrollment image).

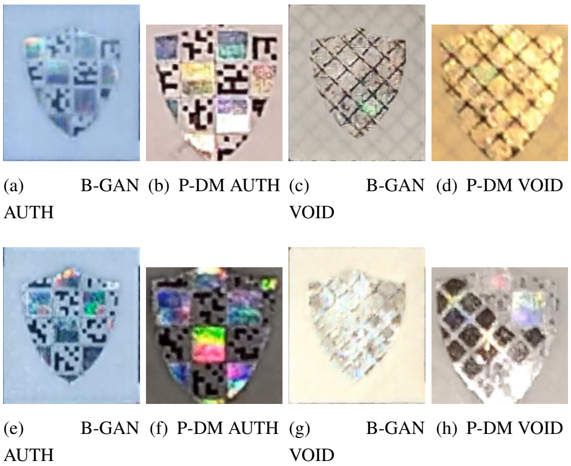

(a) B-GAN AUTH (b) P-DM AUTH (c) B-GAN VOID (d) P-DM VOID

(e) B-GAN AUTH (f) P-DM AUTH (g) B-GAN VOID (h) P-DM VOID

Figure 3: Synthetic images from both classes (AUTH and VOID) and models (B-GAN and P-DM) generated from the enrollment images in Figure 2 (Top row 2(a) and bottom row 2 (d)).

The model performance evaluation is carried out on the real scan images of the test set. The test set is quite imbalanced with respect to the number of images per class (∼27k Authentic scan images and ∼2450 VOID scan images). Hence, we employ evaluation metrics that are suited for imbalanced datasets. As performance measures we compute the per-class accuracy (number of correctly classified images of a given class divided by the number of samples of the given class) and the Balanced accuracy (sum over the per-class accuracies divided by the number of classes (2)). The VOID pattern detector is trained and evaluated 5 times (runs) and we report the means and the standard deviations of the results over the 5 runs.

4 RESULTS

The following section reports the results of the image quality analysis (Sec. 4.1) and the performance of the VOID pattern detector trained on synthetic and real images (Sec. 4.2).

4.1 Image Quality Analysis

In this section, we analyze the quality of the different generators by visually analyzing the image quality and by measuring the Frechet Inception Distance (FID) (Heusel et al., 2017). In Figure 3, some representative image samples generated by both generation methods (i.e., B-GAN and P-DM) are shown. To generate the synthetic scan images, grayscale transformed enrollment images of the original size are used for B-GAN and center cropped enrollment images for P-DM.

Table 1: Frechet Inception Distance (FID) for each generator.

Model	Trained on	Image Size	FID
B-GAN	AUTH	128×128	22.65
B-GAN	AUTH	original	27.47
P-DM	AUTH	128×128	11.64
B-GAN	VOID	128×128	35.52
B-GAN	VOID	original	36.77
P-DM	VOID	128×128	10.97

At the first glance, the generated synthetic images from both image generation methods all look convincing and show image effects that also appear in the real scan images. The B-GAN generated images impress with their diversity. However, at the pixel level one can observe that the B-GAN generated images are more blurry than the original images. Furthermore, there are no B-GAN generated VOID images in which the VOID pattern appears only on small parts of the label (which occurs in some of the real VOID images and also the P-DM generated VOID images). The synthetic images generated by the P-DM are also quite diverse, but not to the same extent than the ones from the B-GAN. In the authors opinion, the quality of the generated images from the P-DM appears slightly better than those from the B-GAN.

The FID scores of each generator are shown in Table 1. Note that in literature, FID scores are mostly used to measure the sample quality of unconditional image generators. However, to measure the FID score of a conditional image generator, the FID score should only depend on the distribution of the scan images and be independent on the underlying enrollment images. Therefore, we create a ground-truth set for FID score computation by randomly sampling 15k real scan images from the AUTH and VOID training set, respectively. We then take the corresponding enrollment image of each scan and generate a synthetic image using the generator. Afterwards, we calculate the FID score between the two sets from the same class, each composed of 15k images.

As can be seen in Table 1, the FID scores obtained by B-GAN trained on AUTH images are lower than on VOID images. This indicates that synthetic AUTH images have a superior quality, which is also inline with our visual observation. A reasonable argument to justify this observation is by the number of samples. While the AUTH generators were trained on $\sim$240k real images, the VOID generators could only be trained on $\sim$20k images due to a lack of real VOID scan images.

Surprisingly, this is not the case for P-DM. In contrast to B-GAN, the P-DM model trained on VOID images achieves a slightly lower FID than the model trained on AUTH images. However, generating some VOID scan images using P-DM for some selected enrollment shows the potential explanation for the low FID score. Figure 4 show a series of VOID images generated by P-DM (bottom row) from a single enrollment image as well as some corresponding real VOID images (top row). As can be seen by comparing both rows, the model seems to have memorized the training images and hence the generated samples lack diversity. Even the VOID pattern in the synthetic images occurs at the same position as in the real images (right bottom part of the hologram). Note that this phenomenon has already been observed before (Carlini et al., 2023).

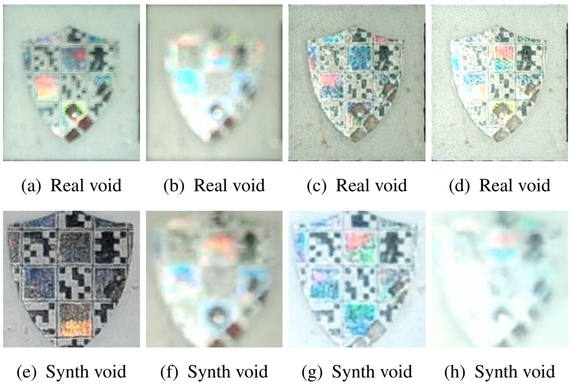
(a) Real void (b) Real void (c) Real void (d) Real void

(e) Synth void (f) Synth void (g) Synth void (h) Synth void

Figure 4: Examples of real and synthetic VOID scan images for chosen enrollment images from the training set. The top row shows the real images. The bottom row shows some synthetic images generated by the P-DM model.

In summary, after inspecting the images visually as well as using FID, images generated by the diffusion model tend to have a better image quality. However, generated images lack diversity and they are more prone to overfitting (this can be observed in particular for the VOID model). Scan images generated by BicycleGAN exhibit a lower quality but are clearly more diverse.

We argue that although overfitting clearly is not ideal, it is not an issue for the subsequent experiment using the VOID pattern detector. In fact, if the generator just learned to copy scan images from the training set, a VOID pattern detector trained on these data should exhibit the same performance as a detector trained on real images. Hence, we expect that scan images produced by the diffusion model should outperform scan images produced by BicycleGAN in the VOID pattern detection evaluation. At least if FID is a useful metric to measure the quality of a dataset for such a task.

4.2 VOID Pattern Detection Results

In Table 2, we present the average results on the test set over 5 runs of training and evaluation of the CNN-

Table 2: Mean VOID detection results and the standard deviations (in brackets).

Data			ACC		
AUTH	VOID	Image Size	AUTH	VOID	Balanced
Real	Real	128×128	0.99 (0.00)	0.84 (0.01)	0.91 (0.01)
Real	Real	original	1.00 (0.00)	0.83 (0.01)	0.91 (0.00)
B-GAN	Real	128×128	0.12 (0.00)	0.98 (0.01)	0.56 (0.02)
B-GAN	Real	original	0.00 (0.00)	1.00 (0.00)	0.50 (0.00)
P-DM	Real	128×128	0.42 (0.00)	0.96 (0.01)	0.76 (0.05)
B-GAN	B-GAN	128×128	0.99 (0.00)	0.69 (0.05)	0.83 (0.02)
B-GAN	B-GAN	original	0.99 (0.00)	0.63 (0.02)	0.81 (0.01)
P-DM	P-DM	128×128	0.88 (0.00)	0.73 (0.03)	0.81 (0.02)

based VOID detection. The CNN is trained either with real scan images, synthetic images, or using real scan images for the class VOID and synthetic images for the class AUTH. As expected, the clearly best results are achieved using only real world training data with a balanced accuracy of 91% for both image sizes. This constitutes the performance baseline, which synthetic images should come close too. Using real world training data from the VOID class and synthetic images for the AUTH class did not work at all for B-GAN and only quite poor for P-DM. When the CNN is trained using synthetic image from one and the same method, then the results are clearly better than for the mixed scenario (B-GAN:81%/83%, P-DM:81%), but still clearly worse than the results using real image data for training.

From the results in Table 2, we can see that the worst classification accuracy is achieved if synthetic training data is used for class AUTH and real training data for class VOID. The fact that using mixed training data produces worse results than using only synthetic images, despite the fact that real-world data produces the best results, leaves only one plausible explanation: The CNN-based VOID detector preferentially learns model-specific features over class-specific features. Such detectors can only fail on the test set, which is composed of real data. This is clearly recognizable when we observe the per-class accuracies for using mixed training data: Nearly all test set images were classified as VOID, the same class that includes the real training data.

So, in case of the mixed training data, the VOID detector primarily learned to differentiate between real and synthetic images, instead of learning to differentiate between the two classes AUTH and VOID as it was supposed to. This means that the synthetic image data is clearly distinguishable from the real images and the differences between real and synthetic data provide a more obvious decision boundary for the VOID detector than class-specific features.

So, the further questions are what are these differences between real and synthetic images and how can these differences be reduced.

5 MODEL-SPECIFIC FINGERPRINTS IN SYNTHETIC DATA

It was shown in previous research (Wesselkamp et al., 2022; Corvi et al., 2023), that synthetically generated images from both GAN and diffusion model based approaches include visible artifacts in the frequency domain and that synthetic and real images exhibit significant differences in the mid-high frequency signal content. These characteristics of synthetic images can be used to identify them as synthetically generated.

We visually highlight the fingerprint of synthetic images from a image generation model in the following way. We randomly select a set of $n = 5000$ real (referred to as R) and synthetic (referred to as S) scan images from one class. Then the fingerprint of the trained image synthesis model is computed as follows:

$$FP(R,S) = \frac{1}{n}\sum_{i=1}^{n}\log(|F(S_i)|) - \frac{1}{n}\sum_{i=1}^{n}\log(|F(R_i)|) \tag{1}$$

where F denotes the Fourier transformation, S_i denotes a synthetic scan image and R_i a real scan image. Taking the logarithm over the absolute valued Fourier transformed image distinctly highlights the artifacts in the frequency domain caused by the image generators. Broadly speaking, the fingerprint is the spectral difference between synthetic images and real images, where ideally all values should be close to zero.

In Figure 5, we present the fingerprints FP of the two employed image generators of both classes. We can observe that the B-GAN fingerprints exhibit a distinct grid pattern. This pattern is most likely a result of the transposed-convolution operation used for upsampling, which is known to cause checkerboard artifacts in the spatial domain (Frank et al., 2020). The B-GAN fingerprints of the two classes are similar from a visual point of view, but there are also clear differences between them. This indicates that the B-GAN models of the two classes generate slightly different model-based image characteristics.

The P-DM FPs do not exhibit the clearly noticeable grid-like pattern like B-GAN FPs (at least it is less prominent). However, there are some other types of repeating pattern. These patterns seem to be characteristic for each class. In any case, there is an obvious difference between the FPs of both classes. We assume that the presence of repeated patterns in the frequency domain of the synthetic images is one of the fundamental reasons why the VOID pattern detector trained on synthetic images performs worse than on real images. Even worse, the pattern that emerges

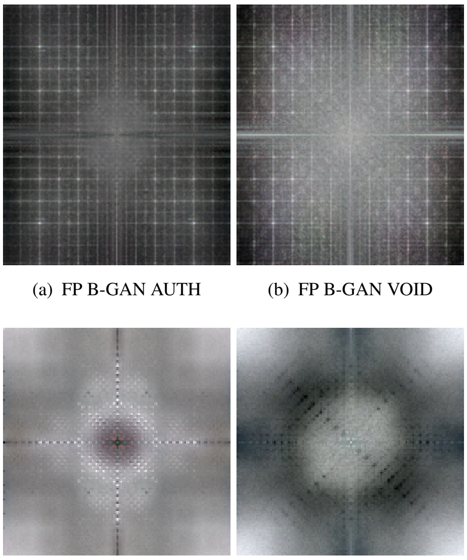

(a) FP B-GAN AUTH (b) FP B-GAN VOID

(c) FP P-DM AUTH (d) FP P-DM VOID

Figure 5: B-GAN and P-DM fingerprints (FP) of synthetic images from the classes VOID and AUTH.

appears to be distinct for each generator and class (note that each fingerprint shown in Figure 5 exhibits a unique pattern). That means that the VOID detector can be easily tempted to classify images using model-based characteristics instead of class-specific characteristics (e.g., the VOID pattern). Since the test set is composed of real images, which do not exhibit such fingerprint, the VOID detector will fail to classify those images. This of course leads to the problem that the VOID detector is not able to properly differentiate between the classes when applied to real scan images, whenever the VOID model is trained at least partly with synthetic data (one class real scan images the other one synthetic images or both classes trained with synthetic images).

To deal with that problem, we employ two methods from the research area of deep fake detection that were presented in (Wesselkamp et al., 2022). The two methods 'Mean-Spectrum Attack' and 'Frequency-Peaks Attack' both aim to remove or lessen the fingerprints on synthetic images. These two methods were employed in (Wesselkamp et al., 2022) to counterattack methods that recognize synthetic images. Roughly explained, the method Mean-Spectrum Attack (MSA) calculates the average difference in the frequency spectrum between synthetic and real images and then subtracts the average difference from each synthetic image in the frequency domain. However, we observed that it is only able to slightly reduce the peaks in the fingerprints as shown in Figure 5. The method Frequency-Peaks Attack (FPA) follows a slightly different strategy and aims to remove the peaks in the frequency domain, that are typically in synthetic images and can be observed in the fingerprints shown in Figure 5. However, we observed that this methods does not only remove peaks but partly changes also other image characteristics like the color and brightness distribution of the images.

Table 3: VOID detection results before and after fingerprint removal using the two methods Mean-Spectral Attack (MSA) and Frequency-Peak Attack (FPA).

	Data		ACC		
FP rem.	AUTH	VOID	AUTH	VOID	Bal.
-	B-GAN	Real	0.12 (0.00)	0.98 (0.01)	0.56 (0.02)
MSA	B-GAN	Real	0.20 (0.00)	0.98 (0.00)	0.62 (0.04)
FPA	B-GAN	Real	0.03 (0.00)	1.00 (0.00)	0.51 (0.01)
-	P-DM	Real	0.42 (0.00)	0.96 (0.01)	0.76 (0.05)
MSA	P-DM	Real	0.20 (0.00)	0.98 (0.00)	0.62 (0.04)
FPA	P-DM	Real	0.03 (0.00)	1.00 (0.00)	0.51 (0.01)
-	B-GAN	B-GAN	0.99 (0.00)	0.69 (0.05)	0.83 (0.02)
MSA	B-GAN	B-GAN	1.00 (0.00)	0.63 (0.02)	0.81 (0.01)
FPA	B-GAN	B-GAN	1.00 (0.00)	0.14 (0.07)	0.57 (0.03)
-	P-DM	P-DM	0.88 (0.00)	0.73 (0.03)	0.81 (0.02)
MSA	P-DM	P-DM	0.37 (0.00)	0.91 (0.04)	0.65 (0.01)
FPA	P-DM	P-DM	0.84 (0.00)	0.27 (0.19)	0.56 (0.04)

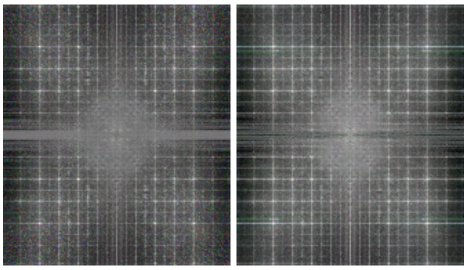

(a) FP B-GAN MSA (b) FP B-GAN FPA

Figure 6: Fingerprints (FP) of B-GAN generated images from the class AUTH after fingerprint removal using the methods MSA and FPA.

In Table 3, we present the results of the VOID detection model (mean and Std (in brackets) over the results of 5 runs) after applying the two fingerprint removal techniques MSA and FPA, compared to the results without fingerprint removal. Unfortunately, it turned out both fingerprint removal methods did not improve the results but even made them worse. Even more so, the fingerprints of synthetic images did hardly change and were still present after the fingerprint removal. This can be observed in Figure 6, where we show the fingerprints of B-GAN generated images after applying the two fingerprint removal techniques to the generated images.

6 CONCLUSION

In this work we analyzed the impact of synthetic training data on a deep-learning based classifier. The classification models were trained either with real, synthetic, or mixed data (one class of real images, the other one with synthetic images). The clearly best classification rates were achieved using only real-world data (91%), followed by using only synthetic data (81-83%), and the worst results were achieved using mixed data (50-76%). A comparison of the frequency spectra of the synthetic images showed that each generator exhibits unique model-specific characteristics (a model-specific fingerprint). It's likely that this fingerprint is one of the reasons for the degraded performance of the classifiers trained on synthetic data and, even more so, on mixed data. In any case, the experiments clearly demonstrate that, despite substantial developments in the field of synthesis, synthetic training data should always be used with caution, especially when synthetic data is used to replace only data of a single class. There is always the risk that a deep learning based classifier learns to differentiate based on model-specific characteristics and not, as intended, based on class-specific features.

The employed FP removal techniques did not work as intended and were unable to bridge the gap between real and synthetic data. In future work, we therefore plan to develop better FP removal techniques.

ACKNOWLEDGEMENTS

This work has been partially supported by the Salzburg State Government within the Science and Innovation Strategy Salzburg 2025 (WISS 2025) under the project AIIV Salzburg (Artificial Intelligence in Industrial Vision), project no 20102-F2100737- FPR.

REFERENCES

Carlini, N., Hayes, J., Nasr, M., Jagielski, M., Sehwag, V., Tramèr, F., Balle, B., Ippolito, D., and Wallace, E. (2023). Extracting training data from diffusion models.

Chen, Y., Yang, X.-H., Wei, Z., Heidari, A. A., Zheng, N., Li, Z., Chen, H., Hu, H., Zhou, Q., and Guan, Q. (2022). Generative adversarial networks in medical image augmentation: A review. *Computers in Biology and Medicine*, 144:105382.

Corvi, R., Cozzolino, D., Poggi, G., Nagano, K., and Verdoliva, L. (2023). Intriguing properties of synthetic images: from generative adversarial networks to diffusion models.

Dhariwal, P. and Nichol, A. (2021). Diffusion models beat gans on image synthesis. *Advances in neural information processing systems*, 34:8780–8794.

Elreedy, D. and Atiya, A. F. (2019). A comprehensive analysis of synthetic minority oversampling technique (smote) for handling class imbalance. *Information Sciences*, 505:32–64.

Frank, J., Eisenhofer, T., Schönherr, L., Fischer, A., Kolossa, D., and Holz, T. (2020). Leveraging frequency analysis for deep fake image recognition. In *International conference on machine learning*, pages 3247–3258. PMLR.

Heusel, M., Ramsauer, H., Unterthiner, T., Nessler, B., and Hochreiter, S. (2017). Gans trained by a two time-scale update rule converge to a local nash equilibrium. *Advances in neural information processing systems*, 30.

Ho, J., Jain, A., and Abbeel, P. (2020). Denoising diffusion probabilistic models. *Advances in neural information processing systems*, 33:6840–6851.

Li, G., Ji, Z., Qu, X., Zhou, R., and Cao, D. (2022). Cross-domain object detection for autonomous driving: A stepwise domain adaptative yolo approach. *IEEE Transactions on Intelligent Vehicles*, 7(3):603–615.

Man, K. and Chahl, J. (2022). A review of synthetic image data and its use in computer vision. *Journal of Imaging*, 8(11).

Qiu, H., Yu, B., Gong, D., Li, Z., Liu, W., and Tao, D. (2021). Synface: Face recognition with synthetic data. In *Proceedings of the IEEE/CVF International Conference on Computer Vision*, pages 10880–10890.

Saharia, C., Chan, W., Chang, H., Lee, C., Ho, J., Salimans, T., Fleet, D., and Norouzi, M. (2022a). Palette: Image-to-image diffusion models. In *ACM SIGGRAPH 2022 Conference Proceedings*, pages 1–10.

Saharia, C., Ho, J., Chan, W., Salimans, T., Fleet, D. J., and Norouzi, M. (2022b). Image super-resolution via iterative refinement. *IEEE Transactions on Pattern Analysis and Machine Intelligence*, 45(4):4713–4726.

Song, Y., Sohl-Dickstein, J., Kingma, D. P., Kumar, A., Ermon, S., and Poole, B. (2020). Score-based generative modeling through stochastic differential equations. *arXiv preprint arXiv:2011.13456*.

Tan, M. and Le, Q. (2019). Efficientnet: Rethinking model scaling for convolutional neural networks. In *International conference on machine learning*, pages 6105–6114. PMLR.

Torfi, A., Fox, E. A., and Reddy, C. K. (2022). Differentially private synthetic medical data generation using convolutional gans. *Information Sciences*, 586:485–500.

Wesselkamp, V., Rieck, K., Arp, D., and Quiring, E. (2022). Misleading deep-fake detection with gan fingerprints. In *2022 IEEE Security and Privacy Workshops (SPW)*, pages 59–65, Los Alamitos, CA, USA. IEEE Computer Society.

Zhang, H., Grimmer, M., Ramachandra, R., Raja, K., and Busch, C. (2021). On the applicability of synthetic data for face recognition. In *2021 IEEE International Workshop on Biometrics and Forensics (IWBF)*, pages 1–6. IEEE.

Zhu, J., Zhang, R., Pathak, D., Darrell, T., Efros, A. A., Wang, O., and Shechtman, E. (2017). Toward multimodal image-to-image translation. *CoRR*, abs/1711.11586.